Applied Surface Science 419 (2017) 540–545

Contents lists available at ScienceDirect

Applied Surface Science

journal homepage: www.elsevier.com/locate/apsusc

Graphene for amino acid biosensing: Theoretical study of the electronic transport

S.J. Rodríguez [a,*], L. Makinistian [c], E.A. Albanesi [a,b]

[a] Instituto de Física del Litoral (CONICET-UNL), Güemes 3450, 3000 Santa Fe, Argentina
[b] Facultad de Ingeniería, Universidad Nacional de Entre Ríos, 3101 Oro Verde (ER), Argentina
[c] Departamento de Física, e Instituto de Física Aplicada (INFAP), Universidad Nacional de San Luis-CONICET, Ejército de los Andes 950, D5700BWS San Luis, Argentina

ARTICLE INFO

Article history:
Received 7 March 2017
Received in revised form 29 April 2017
Accepted 3 May 2017
Available online 8 May 2017

Keywords:
Graphene
Biosensor
Amino acid
Adsorption

ABSTRACT

The study of biosensors based on graphene has increased in the last years, the combination of excellent electrical properties and low noise makes graphene a material for next generation electronic devices. This work discusses the application of a graphene-based biosensor for the detection of amino acids histidine (His), alanine (Ala), aspartic acid (Asp), and tyrosine (Tyr). First, we present the results of modeling from first principles the adsorption of the four amino acids on a graphene sheet, we calculate adsorption energy, substrate-adsorbate distance, equilibrium geometrical configurations (upon relaxation) and densities of states (DOS) for each biomolecule adsorbed. Furthermore, in order to evaluate the effects of amino acid adsorption on the electronic transport of graphene, we modeled a device using first-principles calculations with a combination of Density Functional Theory (DFT) and Nonequilibrium Greens Functions (NEGF). We provide with a detailed discussion in terms of transmission, current–voltage curves, and charge transfer. We found evidence of differences in the electronic transport through the graphene sheet due to amino acid adsorption, reinforcing the possibility of graphene-based sensors for amino acid sequencing of proteins.

1. Introduction

The analysis and quantification of biomolecules is crucial in clinical diagnosis and treatment, for this reason in the last years, the construction of biosensors with biomedical application has gained great importance [1–3]. For building biosensors, it is needed to explore materials with high biocompatibility, sensitivity, selectivity with fast response time, and feasible nanoscale fabrication procedures. Graphene, a single layer of carbon atoms, has exhibited superior physical and chemical properties than other 3D materials, positionning it as a strong candidate for the construction of biosensors [4,5]. This material is characterized as a semi-metal or zero gap semiconductor. As for its electrical properties, it has shown (i) a remarkably high electron mobility at room temperature—with experimentally reported values in excess of 15,000 $cm^2 V^{-1} s^{-1}$ [6]—, (ii) low resistivity (10^{-6} Ω cm), (iii) low Johnson noise, which along with its high electron mobility allow it to be utilized as the channel in a field effect transistor (FET), (iv) high surface area 2620 m^2/g for both sides of graphene [7], and 1310 m^2/g for one-side (e.g., supported on a substrate).

Theoretical and experimental advances in structures of graphene-based nanomaterials reported changes in electronic transport properties of a graphene sheet, due to interactions by covalent or non-covalent forces between graphene and severals organic molecules [8–12]. Viswanathan et al. [13] described an approach for the development of a graphene-based biosensor platform using glucose as an example of target molecule. The presence of external molecules can vary its conductivity and this variation can either be monitored using a simple chemiresistor or by a transistor based sensor. Ohno et al. [14] investigated graphene field-effect transistors (GFETs) for electrical detection of pH and protein adsorptions, the GFETs thus acted as highly sensitive electrical sensors for detecting biomolecule concentrations. Furthermore, smaller molecules have been sensed: dopamine [15], and nucleotides in a DNA chain, among others. Zou et al. [16] reported a DNA sensor based on graphene, the current signals of the four bases guanine (G), adenine (A), thymine (T) and cytosine (C), were separated efficiently. Zhen et al. [17] developed a novel FET nanobiosensor based on a chemical vapor deposition

* Corresponding author.
E-mail address: sindy.rodriguez@ifis.santafe-conicet.gov.ar (S.J. Rodríguez).

http://dx.doi.org/10.1016/j.apsusc.2017.05.031
0169-4332/

(CVD)-grown monolayer of graphene, their sensor turned out ultrasensitive, label-free, and highly specific for detection of DNA.

In order to evaluate the possibility of using graphene as an amino acid sequencer in a protein [18,19], in this work we studied the effects produced by the adsorption of amino acids on the electronic transport properties of a graphene sheet. The study is divided into two parts: (1) equilibrium configuration and charge transfer upon adsorption of four amino acids—histidine (His), Alanine (Ala), aspartic acid (Asp) and tyrosine (Tyr)—on a graphene sheet (throughout the article the optimized (i.e., relaxed) structures are notated as His/grap, Ala/grap, Asp/grap and Tyr/grap). (2) Evaluation of the non-equilibrium transport properties of graphene—probability of transmission and the current–voltage (*I*–*V*) curve—, before and after adsorption.

2. Computational details

All the calculations were performed within a pseudopotentials approach to the Density Functional Theory (DFT), utilizing the code OpenMX3.8 [20,21] and adopting a DFT-D3 approximation for the exchange-correlation potential (DFT-D3 corrections included van der Waals interactions [22,23]). First we studied the adsorption of the four amino acids on graphene: His, Ala, Asp and Tyr, basic, neutral, acid, and aromatic neutral amino acids, respectively. Amino acids are composed of a carboxyl group (—COOH), an amino group ($-NH_2$), and a side-chain (R group), which distinguishes the nature of each amino acid. Subsequently, we modeled a device to study the effects of the molecules on the electronic transport of graphene.

In order to calculate the adsorption energy E^{ads}(eV) and adsorption distance d^{ads}(Å) a set of relaxations were carried. First, for each amino acid (His, Ala, Asp and Tyr), an initial geometry was obtained by optimizing the amino acid structure. Later, with the aim to eventually find the most stable system geometry, the relaxed molecule was located on a graphene sheet at heights and orientations diferents—with and within carboxyl and amine groups parallels to graphene sheet—, and for each atomic arrangement, a total relaxation of the system was carried out (amino acids and graphene atoms). The interaction energy (E_{int}) was calculated according to:

$$E_{\text{int}}(h) = E_{sub-ads}(h) - E_{ref} \quad (1)$$

where the $E_{sub-ads}$ (h), is the energy of the substrate-adsorbate system for each distance (h) and E_{ref} is the total energy when the interaction between substrate-adsorbate system is negligible (there is no interaction between amino acids and graphene when $h = 12.5$ Å). Finally, the E^{ads} is the minimum interaction energy.

A cut-off energy of 180 Ry was used in the numerical integrations and the solution of Poisson equation, and a k-mesh of $5 \times 5 \times 1$ was used for the self-consistency. For the relaxation, the convergence criterion was of 0.02 eV/Å. The charge transfer was calculated from Mulliken population analysis. The electronic density redistribution over the graphene sheet induced by the adsorbed amino acids was defined as:

$$\Delta D = D_{amino.acid+graphene} - D_{amino.acid} - D_{graphene} \quad (2)$$

where D is the charge density.

The effects of the adsorption on the electronic transport properties of graphene were investigated by first-principles calculations within a combination of DFT and Nonequilibrium Green's Functions (NEGF). We defined three regions L, R and C. A central scattering region (C) sandwiched between a semi-infinite source (left, L) and a drain (right, R) electrode regions. We considered infinite left L and right R graphene leads along the *x*-axis under a two-dimensional periodic boundary condition on the *yz* plane (see Fig. 1). The central region C contained the molecules adsorbed on graphene. The

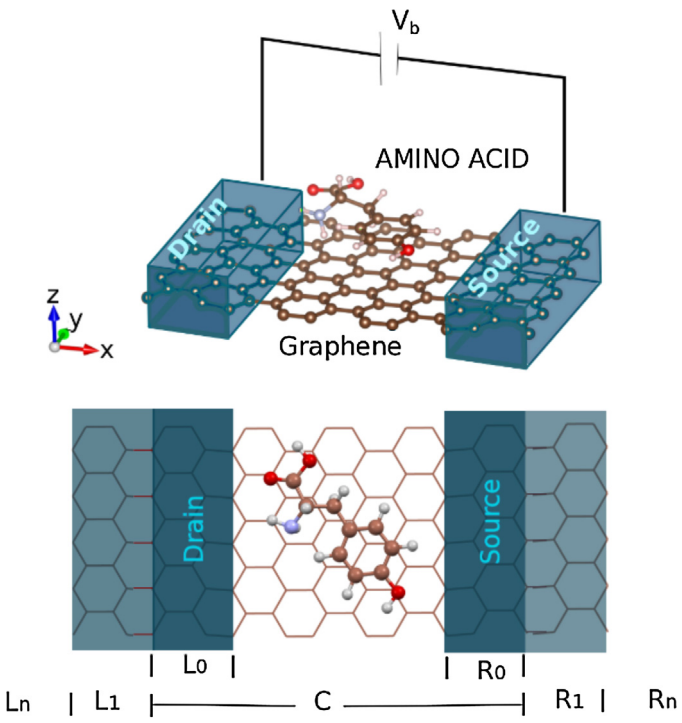

Fig. 1. Configuration of the system treated by the NEGF method, with infinite left and right graphene leads along the *x*-axis under a two-dimensional periodic boundary condition on the *yz* plane. The central region is determined as the equilibrium geometry of amino acids on graphene.

supercell had dimensions $21.30 \times 12.29 \times 25.00$ Å^3 with the two electrode regions containing 20 carbon atoms each, whereas the central (scattering) region contained 60 carbon atoms belonging to graphene, plus the amino acid. The voltage was applied along the *x*-axis, and a temperature of 600 K was used in the Fermi-Dirac distribution, which yields a good compromise between accuracy and efficiency in the implementation of the non-equilibrium Green function method [21].

We modeled five devices: His/grap, Ala/grap, Asp/grap, Tyr/grap and graphene alone. We applied bias voltages (V_b) between the two electrodes of the device in the interval of −2 V to 2 V, with the aim of obtaining the probability of transmission and the current–voltage (*I*–*V*) curve. The transmission probability of electrons incident at an energy E through the device under the potential bias V_b was calculated using Landauer's formula:

$$T(E) = \frac{1}{V_c} \int_{BZ} dk^3 T^k(E) \quad (3)$$

where $T^k(E)$ is the k-resolved transmission, expression within a Green's functions formalism.

The current is evaluated by

$$I = \frac{e}{h} \int dE T(E) \Delta f(E) \quad (4)$$

where $f(E)$ is the difference of Fermi-Dirac distribution functions centered at the electrodes' electrochemical potentials.

3. Discussion of results

3.1. Amino acid adsorption

In Fig. 2 the equilibrium configurations are presented. A tendency to a parallel configuration between rings and graphene is observed for His/grap and Tyr/grap (amino acids His and Tyr have

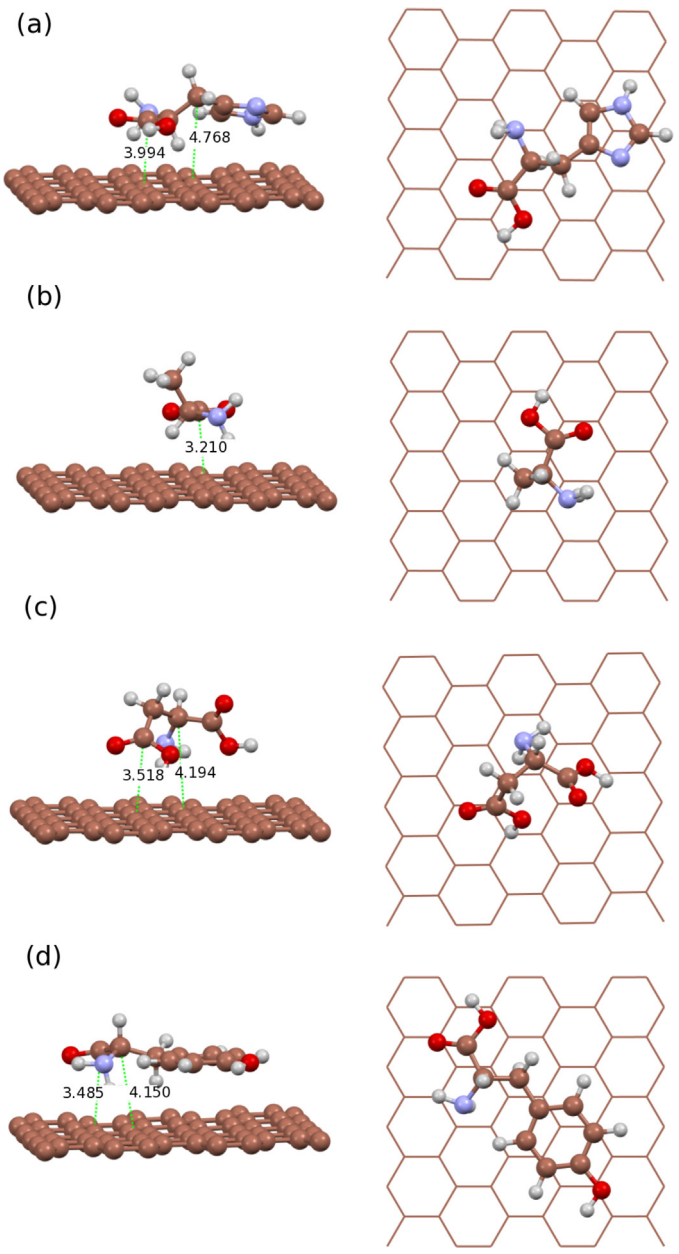

Fig. 2. Equilibrium geometry for amino acids on graphene (a) His/grap, (b) Ala/grap, (c) Asp/grap and (d) Tyr/grap. All distances are in Å.

a side-chain composed of an imidazole ring and a phenol group, respectively). In Tyr/grap the phenol ring is composed of an —OH group, the stronger interaction between the oxygen atom and the graphene sheet generates a completely parallel arrangement between the ring and the graphene sheet. The nature of tyrosine molecules to adopt a flat orientation is consistent with experimental studies on graphene oxide (GO) [7]. A parallel arrangement between the —COOH and —NH_2 groups and the graphene sheet is observed for all systems with minimal energy.

In Table 1 we present E^{ads} and d^{ads} (adsorption distance is measured from the geometric center of the biomolecule to the graphene sheet) for each system. We report that $E^{ads}_{Tyr/grap} > E^{ads}_{His/grap} > E^{ads}_{Asp/grap} > E^{ads}_{Ala/grap}$, whereas $d^{ads}_{Asp/grap} > d^{ads}_{Ala/grap} > d^{ads}_{His/grap} > d^{ads}_{Tyr/grap}$. The systems with the highest E^{ads} present lesser substrate-adsorbate distances (His and Tyr). The amino acids adsorbed on graphene present a strong physisorption with substrate-adsorbate distances

Table 1
Adsorption energy (E^{ads}), adsorption distance (d^{ads}), and transferred charge (Q) for substrate-adsorbate systems: His/grap, Ala/grap, Asp/grap and Tyr/grap.

Gap	Graphene acceptor or donor	Q (e)	d^{ads} (Å)	E^{ads} (eV)	Adsorbate
No	Donor	0.18	2.97	1.49	His
No	Donor	0.10	3.15	0.91	Ala
No	Donor	0.17	4.00	1.17	Asp
No	Donor	0.12	2.89	1.63	Tyr

greater than 2.8 Å —the values calculated for d^{ads} eliminate any chance of covalent bond formation, i.e. chemisorption is not viable.

We report a charge transfer from the graphene sheet to the biomolecules of 0.18 e, 0.10 e, 0.17 e and 0.12 e for, His, Ala, Asp and Tyr, respectively. Graphene is a weak electron donor in all cases. The order of magnitude of transferred charge is in accordance with other works [24]. For instance, graphene donates 0.99 electrons to molecules of 7′70′8′80′-tetracyano-p-quinonedimethane (TNCQ), in this systems, the adsorption opens a gap in the graphene [25]. For smaller adsorbates NO_2 and H_2O 0.09 e and 0.025 e are transferred from the graphene, respectively [26]. The results are shown in Fig. 3. The green regions correspond to $\Delta D > 0$, i.e., higher electron density due to adsorption. The blue regions correspond to $\Delta D < 0$, the lower charge density due to adsorption. The green surfaces are located between the molecule and the graphene sheet; the electrons that participate in π-π interactions cause the charge excess (interaction of the π-orbitals residing on the amino acids and the delocalized p-electrons of graphene). In His/grap, Ala/grap, and Tyr/grap, the transfer charge generates a vertical dipole, with the graphene sheet losing charge and the molecule gaining it, as shown in Fig. 3. The most important effect is a horizontal charge polarization over the graphene sheet forming a local longitudinal dipole. A significant charge density over the graphene sheet coming from the —COOH and —NH_2 groups is displayed by Asp/grab—in this system the local transversal dipole is mainly due to carboxyl and amine groups, breaking with the vertical dipoles symmetry of the other amino acids adsorbed. This result is consistent with studies of the adsorption of benzene rings with carboxyl groups [3,27], whose the interaction with carboxyl groups and graphene is predicted to induce adsorbate dipoles through charge transfer between the molecules and graphene substrates.

We calculated the density of states (DOS) of graphene alone, His/grap, Ala/grap, Asp/grap and Tyr/grap. The solid black line of Fig. 4a displays the well-known DOS for graphene, with its zero gap and zero states at Fermi energy (Diracs points). His, Asp and Tyr amino acids introduce states near the Fermi energy level of graphene at −1.2 eV, −1.8 eV, and −1.3 eV, respectively. These states do not produce an open-gap in graphene. Ala/grap introduces states in E_F: −2.3 eV (states close to typical DOS of graphene alone).

On the other hand, Fig. 4b shows the states-contribution of the —COOH and —NH_2 groups to the total DOS, for each system. In all systems studied, the states at energies −3.8 eV and −2.1 eV are typical contributions of the —COOH (red line with symbols) and —NH_2 (dotted turquoise line) groups, respectively (see arrows in Fig. 4b). The states nearer the Fermi Energy are introduced by the R groups in His/grap and Tyr/grap (systems with greater adsorption energy), while for Ala/graphene the states are introduced by carboxyl and amine groups. Only in the Asp/grap, there are states at energy −3.1 eV due to carboxyl and amino groups, this explains the difference in charge distribution for this system Fig. 3c.

3.2. Electronic transport

In Fig. 5, the transmission for the five systems studied, for V_b = −1, −1.5 and −2 V, is presented, and significant differences in transmission are given for these bias voltage values. The transmis-

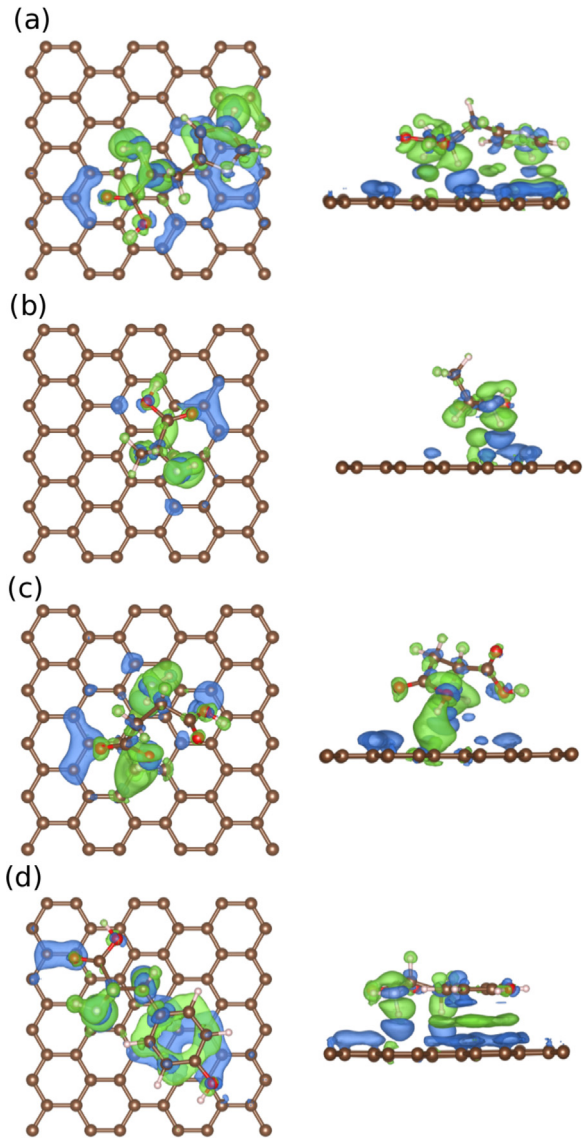

Fig. 3. Charge density. Light grey regions (green color online) accepted electrons ($\Delta D > 0$), while the dark grey regions (blue color online) lost electrons ($\Delta D<0$). (a) His/grap. (b) Ala/graph. (c) Asp/graph. (d) Tyr/grap. (For interpretation of the references to color in this figure legend, the reader is referred to the web version of this article.)

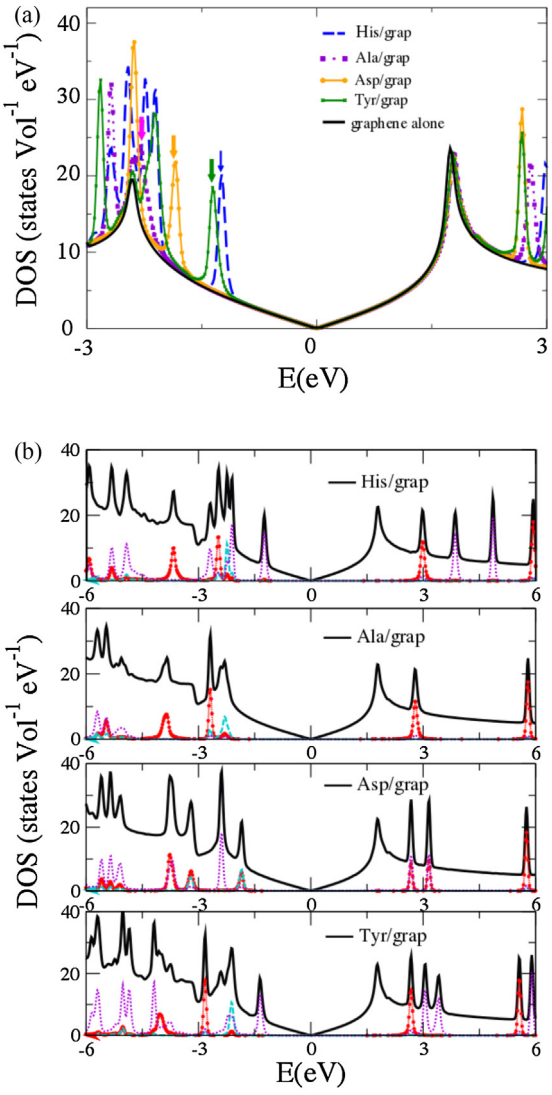

Fig. 4. (a)Total DOS His/grap, Ala/grap, Asp/grap, Tyr/grap and graphene alone. (b) Total DOS His/grap, Ala/grap, Asp/grap and Tyr/grap. Including for each amino acid, the individual contribution to the DOS of the lateral chain (violet dotted lines), the —COOH group (red lines with symbols), and the —NH_2 group (turquoise dashed lines). (For interpretation of the references to color in this figure legend, the reader is referred to the web version of this article.)

sion for adsorbed His, Ala and Asp amino acids (1) increases for V_b = −1, −1.5 and −2 V, (2) is different in comparison to the graphene sheet alone, and (3) is different for each adsorbed amino acid. Tyr amino acid shows an increased transmission for V_b = −1, −1.5 V, but Tyr causes a decrease for V_b = −2 V. Differences in the transmissions of the amino acids are important if a highly selective device is required. The calculated transmissions are in accordance with the current–voltage curves.

Fig. 6 displays the current–voltage (I–V) curve for His/grap, Ala/gra, Asp/grap, Tyr/grap and graphene alone. The I–V curve of the graphene sheet alone exhibits a clear nonlinear behavior, consistent with it being a zero-gap semiconductor. In all systems the value of the current is very low for an applied V_b between −0.5 V and 0.5 V, subsequently, there are significant variations of the current, which depend on each amino acid adsorbed. Between 0.5 V and 2 V the proposed device has the same sensitivity for His and Ala amino acids, this is due to the current corresponding to the His remains close to the current of the Ala. The device has high specificity and sensitivity for V_b between −1 V and −2 V, e.g., for V_b = −1.5 V, the current difference ΔI between each amino acid adsorbed and the graphene sheet is 0.84 μA, 1.05 μA, 1.52 μA, and 0.27 μA for His, Ala, Asp and Tyr, respectively (in Table 2, ΔI for different V_b is reported). The values of ΔI, are in the order of magnitude of the μA. Given that this difference is compared with electrical sensitivity for graphene-based devices, we propose that through measurements of the differential drain-source current, the sensor could detect amino acids in the range of −1 V to −2 V, which could be useful for protein sequence determination (see Table 2).

It is worth mentioning that the electronic response of some materials, particularly the 2D systems, can be improved not only by manipulation of the charge and spin, but also of the valley degrees of freedom [32–34], which result from the anisotropies in a local minimum of the conduction bands, or in a maximum of the valence bands. While this is a plus [35] in carrying and storing information, it requires more complicated sample geometries, magnetic fields, or the use of circularly polarized light to read the additional information. In our case, however, we consider convenient to keep our device as simple as possible, as a sensor driven by just an electric field. Our calculations demonstrate that our standard device

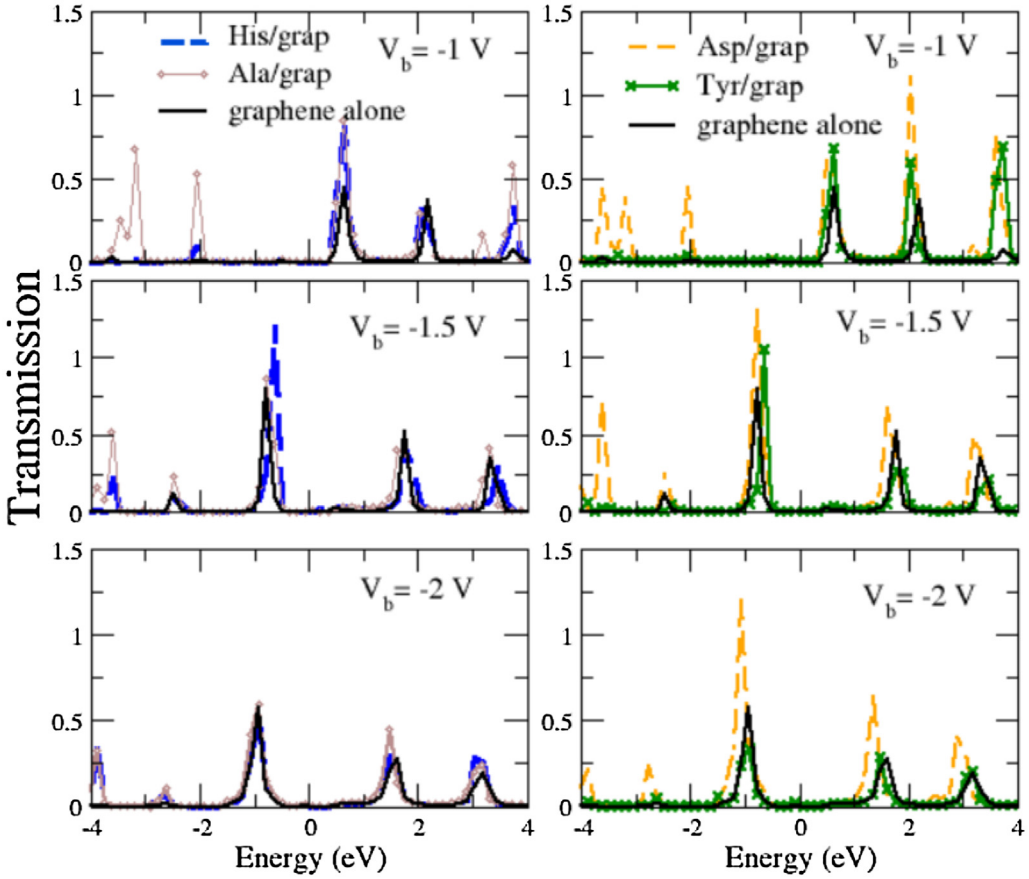

Fig. 5. Transmission for V_b = −1, −1.5 and 2 V for the graphene sheet alone, His/grap, Ala/grap, Asp/grap, and Tyr/grap. In general, the adsorbed amino acid increases transmission, only for Tyr/grap a decrease in transmission at V_b = −2 V is observed.

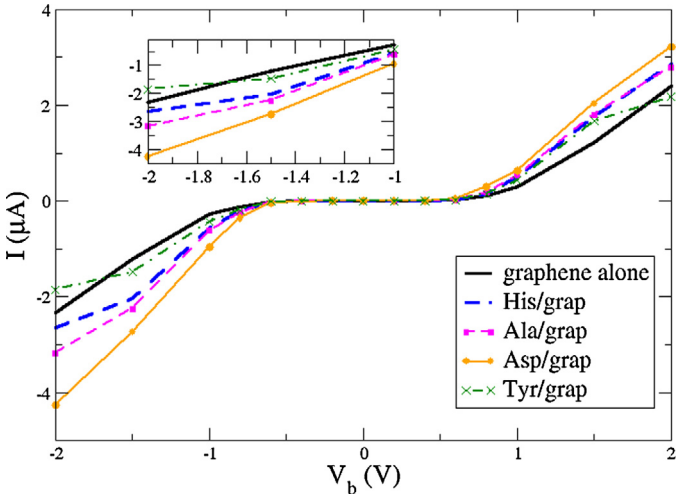

Fig. 6. Current–voltage curves.

Table 2
Our theoretical calculations of current sensibility ($\Delta I = |I_{graphene.alone} - I_{amino.acid.adsorbed}|$) upon amino acid adsorption on graphene (upper part of table). For comparison, we also show (lower part of the table) orders of magnitude of experimentally measured currents on biosensing applications based on graphene FETs available in the literature.

Theoretical graphene-based amino acid biosensing (this work)			
ΔI, μA (V_b = 2 V)	ΔI, μA (V_b = −1.5 V)	ΔI, μA (V_b = −1 V)	Amino acid
0.31	0.84	0.29	His
0.79	1.05	0.37	Ala
1.87	1.52	0.69	Asp
0.46	0.27	0.18	Tyr

Experimental graphene-based devices			
References	I (μA)	Biomolecule	Detected biomolecule
[28]	0.05	Immunoglobulin Ig (G)	Protein
[29]	5	E. coli	Bacteria
[30]	4	DNA	Nucleic acids
[7]	10	DNA	
[31]	1	DNA	

model is highly sensitive to amino acids adsorption for a bias voltage, without the need of using the more sophisticated valleytronic mechanisms.

4. Conclusions

We modeled a graphene-based device for amino acid sensing. The modification of the electronic properties of the graphene sheet through noncovalent functionalization (simple molecular adsorption) is clearly possible. The adsorption process was studied for four amino acids: His, Ala, Asp and Tyr. We report that $E^{ads}_{Tyr/grap} > E^{ads}_{His/grap} > E^{ads}_{Asp/grap} > E^{ads}_{Ala/grap}$, whereas $d^{ads}_{Asp/grap} > d^{ads}_{Ala/grap} > d^{ads}_{His/grap} > d^{ads}_{Tyr/grap}$. The values reported are typical of a strong physisorption.

A transfer of charge from the graphene to the molecules is generated due to the substrate-adsorbate interaction (graphene acts as a weak electronic donor). Local longitudinal and transverse dipoles are induced by the charge transfer toward the adsorbates. In order to evaluate the changes in electronic transport of graphene,

we sandwiched the adsorbed molecule between two graphene electrodes (drain-source). When the V_b applied is between −1 V and −2 V, the modeled device has high specificity and sensitivity for the amino acids His, Ala, Asp and Tyr. The theoretical values for the current are of the same order of magnitude as experimental measurements reported for graphene FET biosensors for other biomolecules. The results suggest the possibility to use a graphene-based biosensor for electrical detection of amino acids, with potential application for a protein sequencer.

Acknowledgements

The authors acknowledge financial support from Consejo Nacional de Investigaciones Científicas y Técnicas (CONICET), through grants PIP 11220150100124 CO (S.J.R. and E.A.A.) and 112-201101-00615 (L.M.). Also, L.M. and E.A.A. acknowledge financial support from the Universidad Nacional de San Luis (PROICO 3-10314), and the Universidad Nacional de Entre Ríos, respectively. The present work used computational resources of the Pirayu cluster, acquired with funds from the Agencia Santafesina de Ciencia, Tecnología e Innovación (ASACTEI). Government of the province of Santa Fe, through the project AC-00010-18, resolution No 117/14. This equipment is part of the National System of High Performance Computing of the Ministry of Science and Technology of the Republic of Argentina.

References

[1] A. Ferrari, Science and technology roadmap for graphene, related two-dimensional crystals, and hybrid systems, Nanoscale 112 (2014) 1–343, http://dx.doi.org/10.1039/C4NR01600A.
[2] T. Kuila, S. Bosea, P. Khanraa, A.K. Mishra, N.H. Kimc, J.H. Lee, Recent advances in graphene-based biosensors, Nanoscale Biosens. Bioelectron. 26 (2011) 4637–4648, http://dx.doi.org/10.1016/j.bios.2011.05.039.
[3] L. Kong, A.E. ans, T.S. Rahman, P.A. Dowben, Recent advances in graphene-based biosensors, J. Phys.: Condens. Matter 26 (2014) 443001, http://dx.doi.org/10.1088/0953-8984/26/44/443001 (27 pp.).
[4] O. Leenaerts, B. Partoens, F.M. Peteers, Graphene Chemistry: Theoretical Perspectives, 1st ed., John Wiley-Sons, 2013.
[5] B. Cai, S. Wang, L. Huang, Y. Ning, Z. Zhang, G. Zhang, Ultrasensitive label-free detection of PNA-DNA hybridization by reduced graphene oxide field-effect transistor biosensor, ACS Nano 8 (2014) 2632–2638, http://dx.doi.org/10.1021/nn4063424.
[6] A. Geim, K. Novoselov, The rise of graphene, Nat. Mater. 6 (2007) 183–191, http://dx.doi.org/10.1038/nmat1849.
[7] S. Mallakpour, A. Abdolmaleki, S. Borandeha, Covalently functionalized graphene sheets with biocompatible natural amino acids, Appl. Surf. Sci. 307 (2014) 533–542, http://dx.doi.org/10.1016/j.apsusc.2014.04.070.
[8] Y. Shao, J. Wang, H. Wu, J. Liu, A. Aksay, Y. Lin, Graphene based electrochemical sensors and biosensors: a review, Electroanalysis 22 (2010) 1027–1036, http://dx.doi.org/10.1002/elan.200900571.
[9] A. Rastkar, B. Ghavami, J. Jahanbin, S. Afshari, M. Yaghoobi, The quantum transport of pyrene and its silicon-doped variant: a DFT-NEGF approach, J. Comput. Electron. 14 (2015) 619–626, http://dx.doi.org/10.1007/s10825-015-0692-2.
[10] H. Vovusha, S. Sanyal, B. Sanyal, Interaction of nucleobases and aromatic amino acids with graphene oxide and graphene flakes, J. Phys. Chem. Lett. 4 (2013) (1929) 3710–3718, http://dx.doi.org/10.1021/jz401929h.
[11] S. Mukhopadhyay, R.H. Scheicher, R. Pandey, S.P. Karna, Sensitivity of boron nitride nanotubes toward biomolecules of different polarities, J. Phys. Chem. Lett. 2 (2011) 2442–2447, http://dx.doi.org/10.1021/jz2010557.
[12] V. Georgakilas, M. Otyepka, A. Bourlinos, V. Chandra, N. Kim, K. Kemp, P. Hobza, R. Zboril, S. Kim, Functionalization of graphene: covalent and non-covalent approaches, derivatives and applications, Chem. Rev. 1 (2012) 1–58, http://dx.doi.org/10.1021/cr3000412.
[13] S. Viswanathan, T.N. Narayanan, K. Aran, K.D. Fink, J. Paredes, P.M. Ajayan, S. Filipek, P. Miszta5, H.C. Tekin, F. Inci, U. Demirci, K.I.B.P. Li, D. Liepmann, V. Renugopalakrishanan, Graphene protein field effect biosensors: glucose sensing, Mater. Today 18 (2015) 513–523, http://dx.doi.org/10.1016/j.mattod.2015.04.003.
[14] Y. Ohno, K. Maehashi, Y. Yamashiro, K. Matsumoto, Electrolyte-gated graphene field-effect transistors for detecting ph and protein adsorption, Nano Letter 9 (2009) 3318–3322, http://dx.doi.org/10.1021/nl901596m.
[15] Y. Wang, Y. Li, L. Tang, J. Lu, J. Li, Application of graphene-modified electrode for selective detection of dopamine, Electrochem. Commun. 11 (2009) 889–892, http://dx.doi.org/10.1016/j.elecom.2009.02.013.
[16] M. Zhou, Y. Zhai, S. Dong, Electrochemical sensing and biosensing platform based on chemically reduced graphene oxide, Anal. Chem. 14 (2009) 5603–5616, http://dx.doi.org/10.1021/ac900136z.
[17] C. Zheng, L. Huang, H. Zhang, Z. Sun, Z. Zhang, G. Zhang, Fabrication of ultrasensitive field-effect transistor DNA biosensors by a directional transfer technique based on CVD-grown graphene, ACS Appl. Mater. Interfaces 7 (2015) 16953–16959, http://dx.doi.org/10.1021/acsami.5b03941.
[18] S. Rodriguez, L. Makinistian, E. Albanesi, Computational study of transport properties of graphene upon adsorption of an amino acid: importance of including —NH_2 and —COOH groups, J. Comput. Electron. 16 (2017) 127–132, http://dx.doi.org/10.1007/s10825-016-0943-x.
[19] P. Singla, M. Riyaz, S. Singhal, N. Goel, Theoretical study of adsorption of amino acids on graphene and BN sheet in gas and aqueous phase including empirical DFT dispersion correction, Phys. Chem. Chem. Phys. 1 (2017) 1–22, http://dx.doi.org/10.1039/C5CP07078C.
[20] T. Ozaki, K. Nishio, H. Kino, Efficient implementation of the non-equilibrium green function method for electronic transport, Phys. Rev. B 81 (2010) 035116, http://dx.doi.org/10.1103/PhysRevB.81.035116.
[21] T. Ozaki, Numerical atomic basis orbitals from h to kr, Phys. Rev. B 67 (2003) 155108, http://dx.doi.org/10.1103/PhysRevB.69.195113.
[22] S. Grimme, J. Antony, S. Ehrlich, S. Krieg, A consistent and accurate ab initio parametrization of density functional dispersion correction DFT-D for the 94 elements h-pu, J. Chem. Phys. 132 (2010) 154104, http://dx.doi.org/10.1063/1.3382344.
[23] S. Grimme, S. Ehrlich, L. Goerigk, Effect of the damping function in dispersion corrected density functional theory, J. Comput. Chem. 32 (2011) 1456, http://dx.doi.org/10.1002/jcc.21759.
[24] O. Leenaerts, B. Partoens, F.M. Peeters, Adsorption of H_2O, NH_3, CO, NO_2, and NO on graphene: a first-principles study, Phys. Rev. B 77 (2008) 125416, http://dx.doi.org/10.1103/PhysRevB.77.125416.
[25] M. Garnica, D. Stradi, S. Barja, F. Calleja, C. D'az, M. Alcami, N. Martin, A.L.V. de Parga, F. Martin, R. Miranda, Long-range magnetic order in a purely organic 2D layer adsorbed on epitaxial graphene, Nat. Phys. 9 (2013) 1, http://dx.doi.org/10.1038/nphys2610.
[26] F. Schedin, S.V.M.A.K. Geim, M.K.E.W. Hill, P. Blake, K. Novoselov, Detection of individual gas molecules adsorbed on graphene, Nat. Mater. 6 (2007) 652, http://dx.doi.org/10.1038/nmat1967.
[27] A. Rochefort, J. Wuest, Interaction of substituted aromatic compounds with graphene, Langmuir 25 (2009) 210–215, http://dx.doi.org/10.1021/la802284j.
[28] S. Mao, G. Lu, K. Yu, Z. Bo, J. Chen, Specific protein detection using thermally reduced graphene oxide sheet decorated with gold nanoparticle-antibody conjugates, Adv. Mater. 22 (2010) 3521–3526, http://dx.doi.org/10.1002/adma.201000520.
[29] Y. Huang, X. Dong, Y. Liu, L. Li, P. Chen, Specific protein detection using thermally reduced graphene oxide sheet decorated with gold nanoparticle-antibody conjugates, J. Mater. Chem. 21 (2011) 12358–12362, doi:0.1039/c1jm11436k.
[30] X. Dong, D. Fu, Y. Xu, J. Wei, Y. Shi, P. Chen, J. Li, Label-free electronic detection of DNA using simple doble-walled carbon nanotube resitors, J. Phys. Chem. 112 (2008) 9891–9895, http://dx.doi.org/10.1021/jp7121714.
[31] M.T. Hwang, P.B. Landon, J. Lee, D. Choi, A.H. Mo, G. Glinsky, R. La, Highly specific SNP detection using 2D graphene electronics and DNA strand displacement, PNA 113 (2016) 201603753, http://dx.doi.org/10.1073/pnas.1603753113.
[32] J. Isberg, M. Gabrysch, J. Hammersberg, S. Majdi, K. Kovi, D. Twitchen, Generation, transport and detection of valley-polarized electrons in diamond, Nat. Mater. 12 (2013) 760–764, http://dx.doi.org/10.1038/NMAT3694.
[33] M.K. Lee, N. Lue, C. Wen, G.Y. Wu, Valley-based field-effect transistors in graphene, Phys. Rev. B 86 (2012) 165411, http://dx.doi.org/10.1103/PhysRevB.86.165411.
[34] F. Chen, M. Chou, Y. Chen, Y.S. Wu, Theory of valley-dependent transport in graphene-based lateral quantum structures, Phys. Rev. B 94 (2016) 075407, http://dx.doi.org/10.1103/PhysRevB.94.075407.
[35] G.Y. Wu, N. Lue, Y. Chen, Quantum manipulation of valleys in bilayer graphene, Phys. Rev. B 88 (2013) 125422, http://dx.doi.org/10.1103/PhysRevB.88.125422.